Intensity impulse response of SDM links

Antonio Mecozzi,[1,*] **Cristian Antonelli,**[1] **and Mark Shtaif**[2]

[1] *Dept. of Physical and Chemical Sciences, University of L'Aquila, 67100 L'Aquila, Italy*
[2] *School of Electrical Engineering, Tel Aviv University, Tel Aviv, Israel 69978*

[*] *antonio.mecozzi@univaq.it*

Abstract: We study the response of space-division multiplexed fiber links to an excitation by a short impulse of the optical intensity. We show that, in the presence of full mixing, the intensity impulse response is Gaussian, confirming recently reported experimental observations, and relate its variance to the mean square of the mode dispersion vector of the link $\vec{\tau}$. The good agreement between our theory and the previously published experiments provides solid foundations to the random coupling model of SDM fiber links, and provides a tool for efficient design of MIMO-DSP receivers.

OCIS codes: (060.2330) Fiber optics communications; (060.4510) Optical communications; (060.4230) Multiplexing; (030.4070) Coherence and statistical optics: Modes.

References and links

1. R. Ryf, S. Randel, A.H. Gnauck, C. Bolle, A. Sierra, S. Mumtaz, M. Esmaeelpour, E.C. Burrows, R. Essiambre, P.J. Winzer, D. W. Peckham, A.H. McCurdy, and R. Lingle, "Mode-Division Multiplexing Over 96 km of Few-Mode Fiber Using Coherent 6 × 6 MIMO Processing," J. Lightwave Technol. **30**, 521–531 (2012). doi: 10.1109/JLT.2011.2174336
2. R. Ryf, R.-J. Essiambre, A. H. Gnauck, S. Randel, M. A. Mestre, C. Schmidt, P. J. Winzer, R. Delbue, P. Pupalaikis, A. Sureka, T. Hayashi, T. Taru, and T. Sasaki, "SDM Transmission over 4200-km 3-Core Microstructured Fiber," OFC 2011, PDP5C.2 (2011).
3. R. Ryf , N.K. Fontaine, B. Guan, R.-J. Essiambre, S. Randel, A. H. Gnauck, S. Chandrasekhar, A. Adamiecki, G. Raybon, B. Ercan, R. P. Scott, S.J. Ben Yoo, T. Hayashi, T. Nagashima, and T. Sasaki, "1705-km Transmission over Coupled-Core Fibre Supporting 6 Spatial Modes," ECOC 2014, Cannes - France, PD.3.2 (2014).
4. R. Ryf, N.K. Fontaine, B. Guan, B. Huang, M. Esmaeelpour, S. Randel, A. H. Gnauck, S. Chandrasekhar, A. Adamiecki, G. Raybon, R.W. Tkach, R. Shubochkin, Y. Sun, and R. Lingle, Jr., "305-km Combined Wavelength and Mode-Multiplexed Transmission over Conventional Graded-Index Multimode Fibre," ECOC 2014, Cannes - France, PD.3.5 (2014).
5. C. Antonelli, A. Mecozzi, M. Shtaif, and P. J. Winzer, "Stokes-space analysis of modal dispersion in fibers with multiple mode transmission," Opt. Express **20**, 11718–11733 (2012).
6. J. P. Gordon and H. Kogelnik, "PMD fundamentals: Polarization mode dispersion in optical fibers," Proc. Natl. Acad. Sci. USA **97**, 4541–4550 (2000).
7. C. Antonelli, A. Mecozzi, and M. Shtaif, "The delay spread in fibers for SDM transmission: dependence on fiber parameters and perturbations," Opt. Express, to be published.
8. The coefficient κ^2 is equivalent to the mean square differential-group-delay (DGD) per kilometer, whose specification is standard in single-mode fiber systems [6].
9. K-P. Ho and J.M Kahn, "Statistics of group delays in multi-mode fibers with strong mode coupling," J. Lightwave Technol. **29**, 3119–3128 (2011).
10. C.W. Gardiner, "Stochastic methods for physics, chemistry and natural sciences," Springer-Verlag, NY, 1983.
11. M. Shtaif and A. Mecozzi, "Study of the frequency autocorrelation of the differential group delay in fibers with polarization mode dispersion," Opt. Lett. **25**, 707–709 (2000).

#231331 - $15.00 USD Received 23 Dec 2014; revised 10 Feb 2015; accepted 11 Feb 2015; published 24 Feb 2015

1. Introduction

Space-division multiplexing (SDM) in fiber optic communications relies on the use of multiple-input multiple-output (MIMO) techniques implemented by means of electronic digital signal processing (DSP). Efficient design of the MIMO DSP algorithms requires knowledge on the statistics of the temporal spreading of the transmitted waveforms, which is determined by the modal dispersion (MD) of the SDM fiber. A convenient and frequently used method for characterizing MD consists of separately exciting each of the spatial channels by a short optical pulse and observing the received intensities in each of the SDM channels [1–4]. In a link operating over a fiber with N spatial modes ($2N$ modes including polarization), this yields $2N \times 2N$ intensity waveforms, whose sum $I(t)$ was used in [2] for assessing the signal delay-spread caused by MD. In this work we show that in the regime of strong mode-coupling and with typical MD values, $I(t) = r(t) \otimes I_0(t)$, where $\otimes$ represents convolution, $I_0(t)$ is the intensity waveform of the pulse that excites the individual SDM channels at the input, and $r(t)$ is what we refer to as the *intensity impulse response* (IIR). We also show that $r(t)$ is a Gaussian function whose mean-square width is given by $\langle|\vec{\tau}|^2\rangle/(2N)^2$, where the angled brackets represent ensemble averaging and where $\vec{\tau}$ is the MD vector which was introduced in [5] as a generalization of the famous polarization mode dispersion (PMD) vector, known in the context of single-mode fibers [6]. As in the case of single mode fibers, the mean square MD value is proportional to the fiber length $\langle|\vec{\tau}|^2\rangle = (2N)^2\kappa^2 L$ [7], where the proportionality coefficient κ^2 is the only relevant parameter for characterizing the delay spread statistics in strongly coupled SDM transmission [8]. The relation between κ and the physical fiber structure is studied in [7]. Since κ can be extracted from experiments such as [1–4], the present analysis has the potential of bridging the gap between system measurements and fiber construction properties.

We stress that contrary to early studies [5, 9], where the delay spread was assumed to be random and equal to the difference between the delays of the slowest and fastest principal modes, in typical SDM fibers the delay spread is deterministic. As we show in this paper, this reality is a consequence of the fact that MD changes substantially across the channel bandwidth, thereby averaging out the randomness of the MD phenomenon.

2. The intensity impulse response

We denote by $\psi_0(t)$ the complex envelope of the pulse used to excite each of the $2N$ modes at the fiber input and by $\tilde{\psi}_0(\omega) = \int_{-\infty}^{\infty} \exp(i\omega t)\,\tilde{\psi}_0(\omega)\mathrm{d}t$ its Fourier transform. In addition, without loss of generality, we assume that $\int_{-\infty}^{\infty}|\psi_0(t)|^2\mathrm{d}t = \int_{-\infty}^{\infty}|\tilde{\psi}_0(\omega)|^2\mathrm{d}\omega/2\pi = 1$. We define a $2N \times 2N$ matrix $\mathbf{H}(t)$ whose j,k element $H_{j,k}(t)$ is the complex envelope of the signal received in the j-th mode, when the k-th mode was excited by $\psi_0(t)$, so that $\mathbf{H}(t)$ is given by

$$\mathbf{H}(t) = \int_{-\infty}^{\infty} \frac{\mathrm{d}\omega}{2\pi} \exp(-i\omega t)\mathbf{U}(L,0;\omega)\tilde{\psi}_0(\omega), \tag{1}$$

where $\mathbf{U}(z,0;\omega)$ is the transfer matrix of the fiber section between the transmitter (assumed to be at $z=0$) and a generic point z. When a given mode k is excited by an impulse at the fiber input, the received power (summed over all output modes) is given by $\sum_{j=1}^{2N}|H_{j,k}(t)|^2$. Similarly to [2–4], our interest in this paper is in the average of this quantity with respect to all the input modes k. Namely, we are looking at

$$I(t) = \frac{1}{2N}\sum_{k=1}^{2N}\left[\sum_{j=1}^{2N}|H_{j,k}(t)|^2\right] = \frac{1}{2N}\mathrm{Trace}\left[\mathbf{H}^{\dagger}(t)\mathbf{H}(t)\right], \tag{2}$$

#231331 - $15.00 USD Received 23 Dec 2014; revised 10 Feb 2015; accepted 11 Feb 2015; published 24 Feb 2015

The Fourier transform of $I(t)$ is readily expressed as

$$\tilde{I}(\Omega) = \int_{-\infty}^{\infty} \frac{\mathrm{d}\omega}{2\pi} \tilde{\psi}_0^*(\omega)\tilde{\psi}_0(\omega+\Omega)\tilde{R}(\Omega,\omega), \tag{3}$$

where

$$\tilde{R}(\Omega,\omega;z) = \frac{1}{2N}\mathrm{Trace}\left[\mathbf{U}(z,0;\omega+\Omega)\mathbf{U}^\dagger(z,0;\omega)\right], \tag{4}$$

and where for the ease of notation we denote $\tilde{R}(\Omega,\omega) = \tilde{R}(\Omega,\omega;L)$. We demonstrate in what follows that in the regime of strong mode coupling, $\tilde{R}(\Omega,\omega)$ can be replaced with its ensemble average $\tilde{r}(\Omega) \equiv \langle \tilde{R}(\Omega,\omega)\rangle$, which is a function of Ω only, owing to the stationarity of the fiber transfer matrix with respect to frequency. In this case the inverse Fourier transform of Eq. (3) yields

$$I(t) = \int_{-\infty}^{\infty} \mathrm{d}t' r(t-t')I_0(t'), \tag{5}$$

where $r(t)$ is the inverse Fourier transform of $\tilde{r}(\Omega)$ and $I_0(t) = |\psi_0(t)|^2$. Equation (5) justifies the choice of referring to $r(t)$ as the IIR.

In order to justify the replacement of $\tilde{R}(\Omega,\omega)$ with $\tilde{r}(\Omega)$ we note that the frequency dependence of the fiber transfer matrix $\mathbf{U}(L,0;\omega)$ is characterized by the correlation bandwidth $B_{\mathrm{MD}} = 2N/\left(2\pi\langle\tau^2\rangle^{1/2}\right) = 1/(2\pi\kappa L^{1/2})$, where we defined $\tau = |\vec{\tau}|$, as we demonstrate in the section that follows. The dependencies of $\mathbf{U}(L,0;\omega+\Omega)\mathbf{U}^\dagger(L,0;\omega)$ and $\tilde{R}(\Omega,\omega) - \tilde{r}(\Omega)$ on ω is characterized by a bandwidth of the same order of magnitude, as long as $\Omega \gg 2\pi B_{\mathrm{MD}}$, namely when $\mathbf{U}(L,0;\omega+\Omega)$ and $\mathbf{U}(L,0;\omega)$ are uncorrelated. Therefore, when the signal bandwidth is much greater than B_{MD}, the contribution of $\tilde{R}(\Omega,\omega) - \tilde{r}(\Omega)$ to the integral in Eq. (3) becomes negligible. As we show later, measurements conducted on state-of-the-art SDM fibers suggest that B_{MD} is of the order of 150MHz [2], whereas typical channel bandwidths in coherent communications are of the order of tens of GHz — more than two orders of magnitudes larger. In the following section we explicitly derive the bandwidth B_{MD} and show that

$$r(t) = \frac{1}{\sqrt{2\pi T^2}}\exp\left(-\frac{t^2}{2T^2}\right), \tag{6}$$

where $T = 1/(2\pi B_{\mathrm{MD}}) = \langle\tau^2\rangle^{1/2}/2N$ is what we refer to as the delay spread [7].

3. Derivation of $r(t)$

The derivation of $r(t)$ follows a procedure similar to the one carried out in [11]. Starting from Eq. (4), we express the forward increment $\mathrm{d}\tilde{r}(\Omega;z) = r(\Omega;z+\mathrm{d}z) - \tilde{r}(\Omega;z)$ as

$$\begin{aligned}\mathrm{d}\tilde{r}(\Omega;z) \quad = \quad & \frac{1}{2N}\left\{\left\langle \mathrm{Trace}[\mathbf{U}(z,0;\omega+\Omega)\mathrm{d}\mathbf{U}^\dagger(z,0;\omega)]\right\rangle + \left\langle \mathrm{Trace}[\mathrm{d}\mathbf{U}(z,0;\omega+\Omega)\mathbf{U}^\dagger(z,0;\omega)]\right\rangle\right. \\ & \left. + \left\langle \mathrm{Trace}[\mathrm{d}\mathbf{U}(z,0;\omega+\Omega)\mathrm{d}\mathbf{U}^\dagger(z,0;\omega)]\right\rangle\right\}. \end{aligned} \tag{7}$$

The increment $\mathrm{d}\mathbf{U}$ can be expressed with the help of Eq. (19) from [5],

$$\mathrm{d}\mathbf{U}(z,0;\omega) = \left[i\frac{\omega\vec{\beta}_\omega\cdot\vec{\Lambda}}{2N}\mathrm{d}z - \frac{\omega^2\kappa^2}{2}\mathrm{d}z\right]\mathbf{U}(z,0;\omega), \tag{8}$$

where the generalized birefringence vector is approximated as $\vec{\beta} = \vec{\beta}_0 + \omega\vec{\beta}_\omega$, and where the immaterial contribution of its frequency independent term $\vec{\beta}_0$ is omitted for simplicity. We assume the strong coupling regime, where $\vec{\beta}_\omega$ is modeled as a $(4N^2-1)$-dimensional isotropic

#231331 - $15.00 USD Received 23 Dec 2014; revised 10 Feb 2015; accepted 11 Feb 2015; published 24 Feb 2015

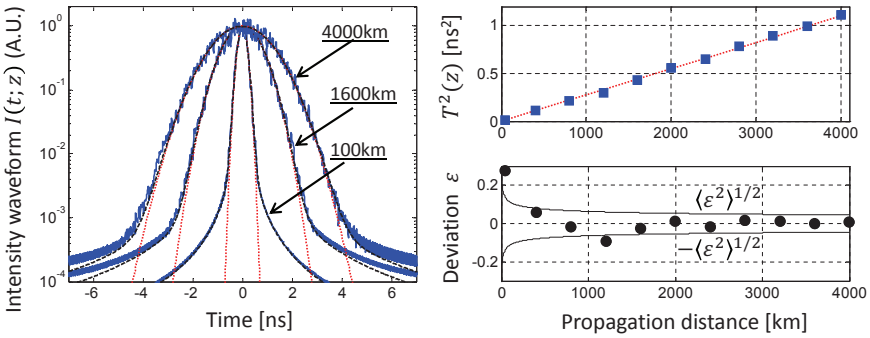

Fig. 1. Left panel: The mode-averaged intensity waveform $I(t;z)$ at several points z along the link obtained by transmitting a Nyquist signal with bandwidth $B = 20$ GHz in the three-core fiber described in [7]. The solid blue curves are the results of simulations, whereas the dashed black curves refer to Eqs. (5) and (6). The red dotted curves correspond to the IIR waveform of Eq. (6) normalized so that their peak value is one. Right top panel: The broadening $T^2(z)$ of the propagating intensity waveform $I(t;z)$ versus propagation distance. The squares show simulation results, whereas the dotted red curve is a plot of $T^2 = \kappa^2 z$ – the temporal mean square width of the IIR waveform. Right bottom panel: Relative deviation of the broadening $T^2(z)$ from the theoretical value, $\varepsilon = [T^2(z) - \kappa^2 z]/\kappa^2 z$, versus propagation distance. The solid thin curves show the standard deviation envelope $\pm\langle\varepsilon^2\rangle^{1/2}$, as given in Eq. (16).

white Gaussian noise process such that $\langle\vec{\beta}_\omega(z)\cdot\vec{\beta}_\omega(z')\rangle = (2N)^2\kappa^2\delta(z-z')$. Equation (8) is a stochastic differential equation that has to be interpreted in the Ito sense, where the second term in the square parentheses is the so-called Ito correction [10]. The modeling of $\vec{\beta}_\omega(z)$ as isotropic delta-correlated noise is an important analytical tool. On the one hand, the strong coupling regime that we consider here (consistently with the majority of reported experiments where quasi-degenerate modes are excited) justifies the assumption of isotropic perturbations. On the other hand, since the correlation length of the actual perturbations is much shorter than the length of the link, the assumption of delta-correlated perturbations is also justified. The coefficient κ, which fully characterizes the perturbations, is determined by the correlation length and the variance of the actual perturbations, as discussed in [7]. We note, however, that although the analysis is performed with delta-correlated perturbations, the simulation results that we present in what follows were performed with a non-zero correlation length. The bandwidth $B_{\rm MD}$ is the width of the autocorrelation matrix $\mathbf{A}(L,\Omega) = \langle\mathbf{U}(L,0;\omega+\Omega)\mathbf{U}^\dagger(L,0;\omega)\rangle$, which owing to the stationary of $\mathbf{U}$ with respect to frequency, is identical to $\mathbf{A}(L,\Omega) = \langle\mathbf{U}(L,0;\Omega)\mathbf{U}^\dagger(L,0;0)\rangle$. As follows from Eq. (8), $\mathbf{U}(L,0;0) = \mathbf{I}$. Therefore $\mathbf{A}(L,\Omega) = \langle\mathbf{U}(L,0;\Omega)\rangle = \exp\left(-\Omega^2\kappa^2 L/2\right)\mathbf{I}$, as is readily obtained from Eq. (8), using the fact that $\langle(\vec{\beta}_\omega\cdot\vec{\Lambda})\,\mathbf{U}(z,0;\Omega)\rangle = 0$. The $\exp(-1/2)$ width of $\mathbf{A}(L,\Omega)$ can be readily verified to be $2\pi B_{\rm MD}$. From the above it readily follows that $\tilde{r}(\Omega) = \mathrm{Trace}\{\mathbf{A}(L,\Omega)\}/2N = \exp\left(-\Omega^2\kappa^2 L/2\right)$, whose inverse Fourier transform is the IIR given in Eq. (6).

In Fig. 1 we test the IIR theory of Eqs. (5) and (6) by considering the three-core fiber example of [2]. Each core's radius is 6.2 μm, the inter-core distance is $d = 29.4\,\mu$m, and the refractive index difference between cores and cladding is of 0.27%. Following up on [7], we assume that perturbations are due to random and independent fluctuations in the three core-to-core distances, as well as due to random polarization coupling in the individual cores. The perturbations are therefore characterized by means of their correlation length L_C, the standard deviation $\Delta b_{\rm rms}$

#231331 - $15.00 USD Received 23 Dec 2014; revised 10 Feb 2015; accepted 11 Feb 2015; published 24 Feb 2015

in the coupling coefficient between each two cores, and in terms of the beat length L_B between polarizations in the individual cores. The numerical settings of the perturbation parameters are those shown in the first row of the table in Fig. 3 of [7], that is $L_B = 20$m, $L_C = 20$m, $b = 2.3$ and $\Delta b_{\rm rms}/b = 0.2$. In the simulation we transmitted a Nyquist signal $\psi_0(t) = \sqrt{B}\sin(\pi Bt)/(\pi Bt)$, with $B = 20$ GHz, over a 4000km link and looked at the mode-averaged intensity waveform $I(t;z)$ at several points z along the link. The numerically obtained waveforms at three specified values of z are plotted by solid blue curves in the left panel of Fig. 1, together with the curves obtained from Eqs. (5) and (6), which are plotted by dashed black curves. The excellent agreement between theory and simulations is self-evident. The red dotted curves, also shown in the figure, correspond to the IIR waveform of Eq. (6) normalized so that their peak value is one. The main lobe of the output intensity waveform is practically identical to the Gaussian-shaped IIR, while only the tails are affected by the shape of the input waveform. This result, which is quite general, is a consequence of the fact that, as occurs in most cases of practical relevance [2–4], the input pulse is much narrower than the IIR, and hence it has little effect on the convolution in Eq. (5). Indeed the intensity waveforms measured in [2–4] were accurately fit by a Gaussian function. In the top right panel of Fig. 1 we show by the blue squares the broadening of the propagating intensity waveform $I(t;z)$, which is denoted by $T^2(z)$ and is defined as the difference between the *temporal* mean-square widths of $I(t;z)$ at point z and at $z = 0$. The dotted red curve is a plot of $\kappa^2 z$ – the temporal mean square width of the IIR waveform. The right bottom panel shows the relative deviation from the theoretical value, $\varepsilon = [T^2(z) - \kappa^2 z]/\kappa^2 z$.

The Gaussian profile of the IIR reflects the Gaussian-shaped spectrum of the correlation function $\tilde{R}(\Omega;z)$, which is a direct consequence of our model, and therefore the agreement with the IIR obtained experimentally in [2] should be interpreted as the model's validation.

4. Accuracy of the delay spread assessment

While the delay spread T, defined by means of Eq. (6) is a deterministic quantity, the actual pulse broadening $T(z)$ depends on the specific instantiation of the SDM fiber and therefore it is in principle a random quantity. In the limit where the bandwidth of the transmitted waveform is much larger than $B_{\rm MD}$, it approaches its average value with negligible fluctuations. In this section we characterize the magnitude of these fluctuations and their dependence on the ratio between the signal bandwidth and $B_{\rm MD}$. To do so, we define the moments of $I(t;z)$ as

$$M_n(z) = \int_{-\infty}^{\infty} t^n I(t;z)\mathrm{d}t = \left(-i\frac{\partial}{\partial\Omega}\right)^n \tilde{I}(\Omega;z)\bigg|_{\Omega=0}, \tag{9}$$

where we remind the reader that $\int_{-\infty}^{\infty} I(t;z)\mathrm{d}t = 1$, which follows from the normalization assumed for $\psi_0(t)$. Using Eq. (3) for $n = 1$ and 2, one obtains

$$M_1(z) = \frac{1}{2N}\int_{-\infty}^{\infty}\frac{\mathrm{d}\omega}{2\pi}\psi_0^*(\omega)\,\mathrm{Trace}\left\{\left[-i\frac{\partial}{\partial\omega}\tilde{\psi}_0(\omega)\mathbf{U}(z,0;\omega)\right]\mathbf{U}^\dagger(z,0;\omega)\right\}, \tag{10}$$

and

$$M_2(z) = \frac{1}{2N}\int_{-\infty}^{\infty}\frac{\mathrm{d}\omega}{2\pi}\mathrm{Trace}\left\{\left[-i\frac{\partial}{\partial\omega}\tilde{\psi}_0(\omega)\mathbf{U}(z,0;\omega)\right]\left[-i\frac{\partial}{\partial\omega}\tilde{\psi}_0(\omega)\mathbf{U}(z,0;\omega)\right]^\dagger\right\}. \tag{11}$$

The frequency dependence of the unitary operator $\mathbf{U}(z,0;\omega)$ is described by [5]

$$-i\frac{\partial}{\partial\omega}\mathbf{U}(z,0;\omega) = \frac{\vec{\tau}(\omega)\cdot\vec{\Lambda}}{2N}\mathbf{U}(z,0;\omega), \tag{12}$$

#231331 - $15.00 USD Received 23 Dec 2014; revised 10 Feb 2015; accepted 11 Feb 2015; published 24 Feb 2015

where we set the mode-independent delay to zero, by assuming ideal chromatic dispersion compensation. Performing the differentiation in the integrand of Eq. (11) and using Eq. (12) we obtain $M_1(z) = M_1(0)$, which we set to zero without loss of generality. Within the same procedure, and assuming a chirp-free input, the pulse broadening $T^2(z) = M_2(z) - M_2(0)$ is found to be

$$T^2(z) = \int_{-\infty}^{\infty} \frac{\mathrm{d}\omega}{2\pi} \frac{|\tilde{\psi}_0(\omega)|^2 \tau^2(\omega)}{(2N)^2}, \tag{13}$$

where $M_2(0) = \int_{-\infty}^{\infty} |\partial \tilde{\psi}_0(\omega)/\partial\omega|^2 \mathrm{d}\omega/(2\pi)$ is the mean square width of the incident pulse $|\psi_0(t)|^2$, and where we used the fact that $\mathrm{Trace}\{[\vec{\tau}(\omega)\cdot\vec{\Lambda}]^2\} = 2N\tau^2(\omega)$ [5]. We now characterize the error $\varepsilon = [T^2(z) - \kappa^2 z]/\kappa^2 z$ by evaluating its variance, using the procedure introduced in [11] for PMD. For the sake of simplicity, we perform the analysis by assuming the same Nyquist pulse used in the previous section. After performing the algebra, one obtains

$$\langle \varepsilon^2 \rangle = \frac{1}{T^4 B^2} \int_{-\pi B}^{\pi B} \frac{\mathrm{d}\omega'}{2\pi} \int_{-\pi B}^{\pi B} \frac{\mathrm{d}\omega''}{2\pi} \frac{\langle \tau^2(\omega')\tau^2(\omega'')\rangle}{(2N)^4} - 1. \tag{14}$$

Using the expression for the correlation function $\langle \tau^2(\omega')\tau^2(\omega'')\rangle$ given in [5] we obtain

$$\langle \varepsilon^2 \rangle = \frac{1}{b^2(4N^2-1)} \int_{-b/2}^{b/2} \mathrm{d}w' \int_{-b/2}^{b/2} \mathrm{d}w'' \, f\left(w' - w''\right) \tag{15}$$

where $f(u) = 4/u^2 - (4/u^4)[1 - \exp(-u^2)]$ and b is a normalized bandwidth $b = \frac{2N}{\sqrt{4N^2-1}} \frac{B}{B_{\mathrm{MD}}}$, so that for N larger than one, $b \simeq B/B_{\mathrm{MD}}$. In the limit of large signal bandwidth $b \gg 1$, the inner integral can be extended to the entire real axis, in which case, using $\int_{-\infty}^{\infty} \mathrm{d}u\, f(u) = 16\sqrt{\pi}/3$, one obtains

$$\langle \varepsilon^2 \rangle \simeq \frac{16\sqrt{\pi}}{3(4N^2-1)b} = \frac{8\sqrt{\pi}}{3N\sqrt{4N^2-1}} \frac{B_{\mathrm{MD}}}{B}, \tag{16}$$

a result consistent for $N = 1$ with the formula given in [11]. As expected, $\langle \varepsilon^2 \rangle$ reduces with the ratio B/B_{MD}, which can be interpreted as the effective number of independent fiber realizations contained in the bandwidth B of the transmitted waveform. For example, in the experiment reported in [2], where $N = 3$, the measured delay spread at $L = 4200$km was $T^2 \simeq 1$ ns^2, and hence $B_{\mathrm{MD}} = 1/(2\pi T) \simeq 160$ MHz, which for the input signal bandwidth $B = 20$ GHz corresponds to a $\langle \varepsilon^2 \rangle^{1/2} \sim 4.5\%$. This small value suggests that the IIR obtained in measurements such as those in [2] is practically deterministic and independent of the particular fiber realization.

5. Conclusion

We studied the response of SDM fiber links to an excitation by a short impulse of the optical intensity, as is commonly performed in experiments [2–4]. We showed that, once the regime of strong mode coupling is achieved, the mode-averaged intensity waveform, referred to as the link's intensity impulse response, becomes a practically deterministic Gaussian shaped function. The IIR's duration is determined by the mode dispersion vector of the link $\vec{\tau}$ which was introduced in [5]. The excellent agreement between the presented theory and published experimental results validates random mode coupling model and provides a tool for efficient design of MIMO-DSP receivers.

Acknowledgement

A. Mecozzi and C. Antonelli acknowledge financial support from the Italian Ministry of University and Research through ROAD-NGN project (PRIN2010-2011). M. Shtaif acknowledges financial support from Israel Science Foundation (grant 737/12).

#231331 - $15.00 USD Received 23 Dec 2014; revised 10 Feb 2015; accepted 11 Feb 2015; published 24 Feb 2015